J Low Temp Phys (2013) 170:302–306
DOI 10.1007/s10909-012-0689-1

Effects of Magnetic-Field Annealing on the Morphology and Magnetic Properties of $La_{0.7}Sr_{0.3}MnO_3$ Film

Z.F. Zi · Q.C. Liu · X.W. Tang · J.G. Lv · J.M. Dai · Y.P. Sun

Received: 10 June 2012 / Accepted: 4 August 2012 / Published online: 21 August 2012

Abstract $La_{0.7}Sr_{0.3}MnO_3$ (LSMO) films were prepared by the chemical solution deposition method with an external magnetic-field ($H_{ext} = 5$ kOe) annealing process. Structural and magnetic properties were systematically investigated. X-ray diffraction results show that both LSMO films are single-phase. The results of field-emission scanning electronic microscopy show that the mean grain size of the film annealed under $H_{ext} = 5$ kOe are about 2.5 times larger than that of the annealed film under $H_{ext} = 0$ kOe. The enhanced magnetic properties are explained reasonably by the magnetic-field annealing.

Keywords $La_{0.7}Sr_{0.3}MnO_3$ film · Magnetic-field annealing · Magnetic properties

1 Introduction

Hole-doped perovskite manganites $La_{1-x}Sr_xMnO_3$ have received a great deal of interest due to their fascinating physical properties, including colossal magnetoresistance (CMR), insulating to metal transition, and paramagnetic to ferromagnetic

Z.F. Zi (✉) · J.G. Lv
Laboratory of Materials Physics, School of Electronic and Information Engineering, Hefei Normal University, Hefei 230601, P.R. China
e-mail: zfzi@issp.ac.cn

Z.F. Zi · Q.C. Liu · J.M. Dai
School of Physics and Electronic Information, Huaibei Normal University, Huaibei 235000, P.R. China

J.M. Dai
e-mail: jmdai@issp.ac.cn

Q.C. Liu · X.W. Tang · J.M. Dai · Y.P. Sun
Key Laboratory of Materials Physics, Institute of Solid State Physics, Chinese Academy of Sciences, Hefei 230031, P.R. China

transition [1–4]. $La_{0.7}Sr_{0.3}MnO_3$ (LSMO) possesses higher value of Curie temperature than room temperature and combines its low carrier density among perovskite-structured $La_{1-x}Sr_xMnO_3$ systems. It is already explained that the double exchange (DE) interaction between pairs of Mn^{3+} and Mn^{4+} ions through an oxygen atom is responsible for its metallic and ferromagnetic properties [5].

It is well-known that the material should be in the form of films from the viewpoint of practical applications. Therefore, in recent years, LSMO films have stimulated intense study because it is widely recognized as one of the most attractive and potential candidates for high-performance room-temperature tunneling magnetic resistance devices due to the almost 100 % spin polarization of charge carriers [6–8]. In particular, integrating LSMO onto Si, the essential material of the semiconductor industry, is crucial in maximizing their potential use. However, the growth of high-quality film on Si substrate is technologically complicated due to the lattice misfit at the interface. Some groups have attempted to prepare LSMO films by some methods, including the pulsed-laser deposition method [9, 10], the DC-magnetron sputtering technique [11]. These results suggest that when LSMO film is required for device integration, the direct growth on Si substrate can be difficult to achieve. Recently, some researchers reported enhanced magnetic properties in $BiFeO_3$ thin films with an applied magnetic-field annealing [12, 13] and Zn-Mn-Zr spinel ferrite thin films [14]. However, there is no report about LSMO films prepared via chemical solution deposition (CSD) method with magnetic-field annealing process. In addition, CSD method not only can be easily used to fabricate LSMO films with large area, but also it is safe to our environment.

In this study, LSMO films were prepared using CSD method by the application of the external magnetic field during annealing. In order to confirm the effect of external magnetic field, LSMO films were prepared with and without the external magnetic field, respectively. The structural, morphological, and magnetic properties of LSMO films were discussed using XRD, FE-SEM and magnetization measurements.

2 Experimental

LSMO films were fabricated on n-type (100)-oriented Si substrates by the CSD method (denoted LSMO/Si). The starting materials of high-purity lanthanum acetate [$La(CH_3COO)_3{\cdot}5H_2O$, 99 %, Alfa Aesar], strontium acetate [$Sr(CH_3COO)_2{\cdot}1/2H_2O$, 99 %, Alfa Aesar], and manganese acetate [$Mn(CH_3COO)_3{\cdot}6H_2O$, 99 %, Alfa Aesar] were dissolved in propionic acid at 70 °C and stirred at this temperature for 20 min. Polyethylene glycol (PEG, molecular weight 20000) was used as surfactant to prevent the colloidal particles of chelate from aggregating. The transparent solution with brown color was further stirred at room temperature for 20 h in order to get well-mixed solution. The total concentration of the metal ions was 0.2 M. The films were synthesized by spin-coating method on Si (100) substrates using rotation speed of 4000 rpm and time of 60 s, and then dried at 300 °C for 5 min to expel the organisms. The spin-coating and dry procedures were repeated four times in order to obtain the film with desired thickness. Some dried film was annealed at 800 °C in air for 20 min in order to get the crystallized film, the others were annealed at 800 °C for 20 min with an external magnetic field ($H_{ext} = 5$ kOe).

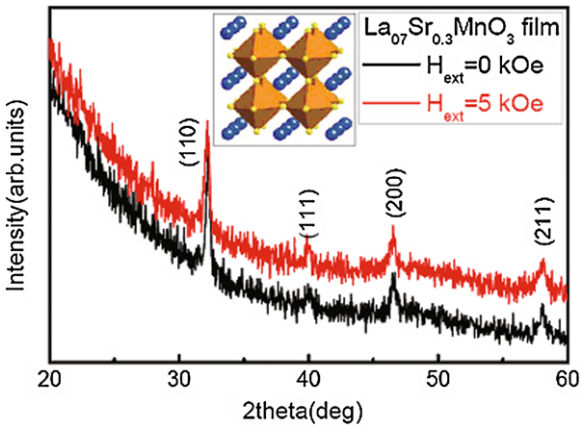

Fig. 1 XRD patterns for the LSMO films annealed without ($H_{ext} = 0$ kOe) and with an external magnetic field ($H_{ext} = 5$ kOe). *Inset*: crystal structure sketch map of perovskite LSMO manganite (Color figure online)

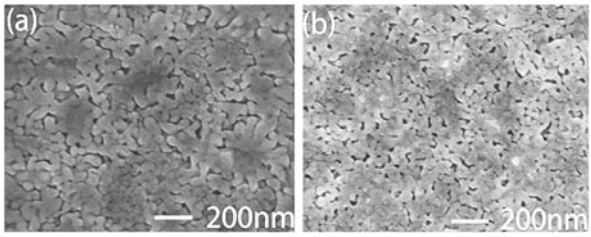

Fig. 2 FE-SEM micrographs of the LSMO films annealed (**a**): $H_{ext} = 5$ kOe and (**b**): $H_{ext} = 0$ kOe

The crystal structure was characterized by X-ray diffractometer (XRD, Philips designed, X'pert PRO type) with Cu radiation (wavelength $\lambda = 1.54056$ Å) at room temperature. The morphology and thickness of the films were investigated by field-emission scanning electronic microscopy (FE-SEM, FEI designed, Sirion 200 type). Magnetization measurements were conducted with a SQUID magnetometer (MPMS, Quantum design).

3 Results and Discussions

The standard XRD θ–2θ patterns of LSMO films annealed without and with an external magnetic field are shown in Fig. 1. All the diffraction peaks of both samples can be well indexed to an orthorhombic structure. The average crystallite size of LSMO particles was estimated using the classical Scherrer formula [15]. The obtained average crystallite sizes of both LSMO films are about 21.6 nm.

To further investigate the effects of magnetic-field annealing on the microstructure, the surface morphologies of the LSMO films have been characterized by FE-SEM images. Figure 2(a) indicates that most of the grains on the surface of the LSMO films are nearly peanut-like and these peanut-like grains exhibit a small size distribution. For LSMO film annealed with an external magnetic field ($H_{ext} = 5$ kOe), peanut-like grains with a diameter of about 50.4 nm and the length of about 116.8 nm. Whereas the grains in Fig. 2(b) annealed without an external magnetic field show 2.5 times smaller diameter and length than those with an external magnetic field. The growth

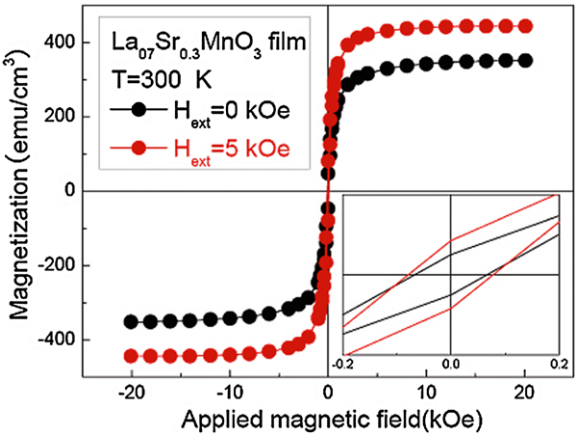

Fig. 3 Room-temperature M(H) hysteresis loops of LSMO/Si annealed under $H_{ext} = 0$ and 5 kOe, respectively, the *inset* exhibits $M(H)$ hysteresis loops on a larger scale (Color figure online)

of larger grains annealed with $H_{ext} = 5$ kOe can be mainly attributed to easy connection, diffusion and agglomeration of individual grains along the annealing magnetic-field direction [16]. The thicknesses of the films detected by the cross-sectional FE-SEM are about 300 nm and the film thickness is independent of the magnetic-field annealing.

In order to investigate the influence of the magnetic-field annealing on magnetic properties of LSMO films, the magnetic field dependence of magnetization curves $M(H)$ are measured under the applied magnetic fields from -20 to 20 kOe, which are parallel to the film plane. The magnetization $M(H)$ hysteresis loops at 300 K for LSMO films are shown in Fig. 3. It is seen that both LSMO films exhibit hysteresis behavior in the $M(H)$ curves, indicating the characteristic of ferromagnetism.

For the LSMO film annealed under $H_{ext} = 5$ kOe, the value of saturation magnetization (M_s) comes out to be 447.0 emu/cm^3, which is higher than that (354.9 emu/cm^3) of the film annealed under $H_{ext} = 0$ kOe. The increased M_s is mainly ascribed to the enhanced magnetic coupling based on above discussion. As seen from the inset of Fig. 3, the coercivity of the magnetic-field annealing film is obviously higher than that of the nonmagnetic-field annealing film since the grain size has a large influence on H_c of the LSMO film, that is, considering our FE-SEM results H_c will increase with an increase in grain size according to Herzer's random anisotropy model [17]. These results demonstrate that the magnetic-field annealing would be a novel and effective method to improve magnetic properties of magnetic films.

4 Conclusions

In summary, magnetic-annealing effects on LSMO thin films prepared via the CSD method are systematically investigated. It is observed that the grain size of LSMO/Si film becomes larger after magnetic-field annealing, which is attributed to the enhancements in the connection and diffusion of components under an external magnetic field. Under the effect of external magnetic field ($H_{ext} = 5$ kOe), M_s of LSMO film

is enhanced, which can be explained by the influence of magnetic texture, released tensile strain and the enlarged grain size.

Acknowledgements This research was financially supported by the National Nature Science Foundation of China (Grant Nos. 51002156, 11274314, 51102072 and 10874051), the Natural Science Major Foundation of Anhui Provincial Higher Education Institutions of China (Grant No. KJ2012ZD14), Anhui Provincial Natural Science Foundation, China (Grant No. 11040606M56), and Annual Scientific Research Plan Key Projects of Anhui Province, China (Grant No. 09020204031).

References

1. M. Mathews, E.P. Houwman, H. Boschker, G. Rijnders, D.H.A. Blank, J. Appl. Phys. **107**, 013904 (2010)
2. M. Veis, S. Visnovsky, P. Lecoeur, A.M.H. Gosnet, J.P. Renard, P. Beauvillain, W. Prellier, B. Mercey, J. Mistrik, T. Yamaguchi, J. Phys. D, Appl. Phys. **42**, 195002 (2009)
3. H.Y. Gao, M. Staruch, M.K. Jain, P.X. Gao, P. Shimpi, Y.B. Guo, W.J. Cai, H.J. Lin, Appl. Phys. Lett. **98**, 123105 (2011)
4. C. Martíez-Boubeta, Z. Konstantinovic, L. Balcells, S. Estrade, J. Arbiol, A. Cebollada, B. Martinez, Cryst. Growth Des. **10**, 1017 (2010)
5. J. Hemberger, A. Krimmel, T. Kurz, H.A. Krug von Nidda, V.Y. Ivanov, A.A. Mukhin, A.M. Balbashov, A. Loidl, Phys. Rev. B, Condens. Matter **66**, 094410 (2002)
6. S.M. Wu, S.A. Cybart, P. Yu, J.X. Zhang, R. Ramesh, R.C. Dynes, Nat. Mater. **9**, 756 (2010)
7. A. Rebello, R. Mahendiran, Appl. Phys. Lett. **96**, 032502 (2010)
8. C. Zandalazini, P. Esquinazi, G. Bridoux, J. Barzola-Quiquia, H. Ohldag, E. Arenholz, J. Magn. Magn. Mater. **323**, 2892 (2011)
9. W. Zhang, I.W. Boyd, N.S. Cohen, Q.T. Bui, Q.A. Pankhaurst, Appl. Surf. Sci. **109–110**, 350 (1997)
10. A.K. Pradhan, D. Hunter, T. Williams, B. Lasley-Hunter, R. Bah, H. Mustafa, R. Rakhimov, J. Zhang, D.J. Sellmyer, E.E. Carpenter, D.R. Sahu, J.L. Huang, J. Appl. Phys. **103**, 023914 (2008)
11. Z.G. Sheng, Y.P. Sun, X.B. Zhu, B.C. Zhao, R. Ang, W.H. Song, J.M. Dai, Solid State Commun. **141**, 239 (2007)
12. W.J. Lou, D.L. Wang, F.W. Wang, T. Liu, J.W. Cai, L.Y. Zhang, Y.L. Liu, Appl. Phys. Lett. **94**, 202507 (2009)
13. S. Anjum, M.S. Rafique, M. Khaleeq-ur-Rahaman, K. Siraj, A. Usman, A. Ahsan, S. Naseem, K. Khan, J. Cryst. Growth **324**, 142 (2011)
14. X.W. Tang, J.M. Dai, X.B. Zhu, H.C. Lei, L.H. Yin, W.H. Song, Y.L. Cheng, D.J. Wu, Y.P. Sun, J. Magn. Magn. Mater. **322**, 2647 (2010)
15. M.I. Mendelson, J. Am. Ceram. Soc. **52**, 443 (1969)
16. M.S. Rafique, M. Khaleeq-ur-Rahman, I. Riaz, R. Jalil, N. Farid, Laser Part. Beams **26**, 217 (2008)
17. G. Herzer, Scr. Metall. Mater. **33**, 1741 (1995)